

Experimental investigation of flow-induced sound of kite lines

Lukas Saur^{1,*}, Jörg Riedel¹, Storm Dunker², and Stefan Becker¹

¹Institute of Fluid Mechanics, Friedrich-Alexander-University Erlangen-Nuremberg, 91054 Erlangen, Germany

²A-Z Chuteworks LLC, Houston, TX 77043, United States

Received 28 November 2022, Accepted 7 June 2023

Abstract – In times of increasing importance of renewable energies, airborne wind energy (AWE) systems represent an emerging extension to conventional wind turbines. Many AWE systems use powerful kites to provide tether traction to mechanically unwind the tether, generating electricity on the ground. In addition to the traction tether, a large number of kite lines spanning the kite are moved through the air at high speed. This can produce a loud unpleasant whistling noise on the ground, which is due to a superposition of the aeolian tones of the many different lines. In the present work, differently structured kite lines were investigated in the aeroacoustic wind tunnel with respect to their sound radiation when they were exposed to a flow at up to 34 ms^{-1} resulting in $\text{Re} \leq 7300$ and angles of attack (AOA) in the range of $90^\circ \geq \text{AOA} \geq 45^\circ$. It was found that greater surface roughness increases sound radiation while line tension has negligible influence. By weaving a single-helix-shaped protrusion into the sheath of the kite line, the total radiated sound pressure level can be reduced by up to 9 dB. If the line itself has a helical contour, even a reduction of up to 11.5 dB is reachable. For decreasing AOA the noise suppression effect of helical surface protrusions and helical line shape is significantly reduced. The results provide initial guidelines on how to effectively reduce sound radiation from aircraft kites. Further investigations should consider the individual contributions of fluid and structural sounds to the total radiated sound of a flying kite.

Keywords: Flow-induced noise, Kite lines, Helical surface protrusions, Strouhal frequency, Noise control

Nomenclature

AOA	angle of attack, °
AWE	airborne wind energy
ν	kinematic air viscosity, $\text{m}^2 \text{ s}^{-1}$
D	test object diameter, mm
f_{St}	frequency of peak sound pressure level, Hz
h	height of helical surface protrusion, mm
HMPE	high-modulus polyethylene
L	test object length, mm
λ	pitch of helical surface protrusion
OASPL	overall sound pressure level, dB(A)
PSPL	peak sound pressure level, dB(A)
Re	Reynolds number
St	Strouhal number
θ	angle of attack, °
VIV	vortex-induced vibrations
U	free stream velocity, ms^{-1}

1 Introduction

Fighting climate change is considered the greatest challenge in the 21st century. In order to reduce CO_2 emissions, it is crucial to replace fossil fuel energy sources with

renewable energy sources. Wind energy offers the greatest expansion potential, especially at higher altitudes where winds become steadier, stronger and more persistent [1]. AWE systems seek to harvest this resource.

Crosswind kite energy systems rely on periodic motions of a tethered kite to obtain greater apparent wind speed than the absolute wind relative to the ground. Such apparent wind generates a high lift force on the kite, which can be exploited to produce power by electric generators on the ground [1, 2]. Currently available kite energy systems are able to generate up to 200 kW electrical output and reach kite speeds of up to 40 ms^{-1} [3].

A loud whistling tone may be heard around the operating area of the kite. This tonal noise is the flow-induced sound resulting from the kite bridles (lines) travelling through an air medium. Kite bridles connect the textile fabric of the kite sail with the strong tether transmitting the lift forces to the ground station. As an example, a 90 m^2 kite sail can have more than 600 m of kite bridles to support the loads generated and to control its shape and stability. The objective of the subject research is to evolve renewable energy technology, specifically as related to AWE and kites, and to increase acceptance and adoption by reducing the audible footprint of kite systems.

In the 19th century, Strouhal [4] found that vortex shedding on cross-flowed cylinders produces a tonal noise, the so

*Corresponding author: lukas.saur@fau.de

called aeolian tone, whose frequency corresponds to the Strouhal frequency. Lighthill [5] classified flow around cylinders as a dipole sound source. Cylinder noise is primarily generated by the unsteady vortex shedding phenomenon causing large pressure fluctuations at the cylinder surface [6, 7]. In the Reynolds number range of interest $800 \leq \text{Re} \leq 7300$, a laminar boundary layer is present on cross-flowed cylinders, which detaches shortly before the thickest point of the body and rolls in to form a periodic vortex formation [8]. Behind the cylindrical test object, a fully turbulent vortex street is formed [9]. The thickness of the laminar boundary layer increases with increasing surface roughness [10]. Alomar et al. [11] showed that greater surface roughness leads to higher sound pressure levels of cross-flowed cylinders. Gerrard [12] carried out sound measurements on circular cylinders in air flows and determined an influence of cylinder vibrations on sound radiation.

The effect of the angle of attack between flow direction and the cylinder axis on the vortex shedding noise can be estimated by applying the independence principle [13]. It assumes that the incident flow speed for an inclined cylinder is the component of the freestream flow speed U_∞ perpendicular to the inclined cylinder centreline $U_n = U_\infty \sin(\theta)$.

Latorre Iglesias et al. [14] assessed the effect of the angle of attack and flow speed on the aerodynamic cylinder noise and compared his results to the experimental studies of Yamada et al. for AOA up to 45° [15], Haramoto et al. up to 40° [16] and King and Barsikow up to 30° [17]. In a Reynolds range of $15.500 \leq \text{Re} \leq 39.000$ and for $30^\circ \leq \text{AOA} \leq 90^\circ$ he found that amplitude and frequency of the aeolian tone and the overall sound pressure level decrease with declining AOA while the bandwidth of the spectral peak increases. The directivity of the vortex shedding noise radiated by circular cylinders was found to be close to that expected for a theoretical dipole source while it is independent of the angle of attack.

A great number of passive noise control methods for circular cylinders were proposed in the past decades, aiming at eliminating or suppressing the vortex shedding phenomenon to reduce cylinder noise. These methods are based on changes in the cylinder surface and include, among others, porous coatings and helical cables wrapped around the cylinder. For kite lines omnidirectional measures are preferred, as lines can twist.

Sueki et al. [18] measured a reduction in radiated sound by applying porous cylinder coatings that can suppress unsteady motion of vortices.

The technique of wrapping helical cables on circular cylinders generates helical surface protrusions (Helix) and functions similar to other 3-D control methods. 3-D near-field flow features caused by the variational cross-section along the cylinder span are preventing the two-dimensional (2-D) nature of the vortex shedding process, leading to weaker vortices in farther distance to cylinder surface [19, 20]. Decreasing pressure fluctuations at the cylinder surface result in lower sound radiation of tonal frequencies while broadband flow noise is reduced due the decrease in velocity fluctuations in the wake [21].

Razali et al. [22] achieved a reduction of vortex-induced vibrations of 98% by wrapping a cylinder with three wires (pitch $\lambda = 10D$, height $h = 0.12D$). The correlation length of the vortices along the cylinder axis is reduced by 75% with respect to the helix. Xing et al. [23] varied pitch and number N of helical cables wrapping along cylinder span, aiming at optimal farfield noise reduction. Helix configurations with $2 \leq N \leq 4$ cable threads wrapped with pitch $1D \leq \lambda \leq 4D$ effectively suppressed both tonal and broadband noise leading to 17 dB reduction of the overall sound pressure level.

Helical surface protrusions for aerodynamic noise reduction were also successfully applied on transmission lines. Tsujimoto et al. [24] performed an experimental study to find the optimum cross section shape for suppression of the aeolian tone of transmission lines. Aeolian noise levels could be sufficiently reduced if the transmission line surface is smoothened and the two helical surface protrusion have a height of $h \geq 0.028D$. With a protrusion height of $h = 0.07D$ a peak sound pressure level reduction of 10 dB was achieved.

Flexible, tensioned kite lines in cross-flow are susceptible to vibrations with the vortex shedding frequency. First investigations of the influence of helical surface protrusions on the aerodynamic behaviour on long flexible structures like kite lines have been conducted by Dunker et al. [25]. Kite lines with helical surface protrusions were developed to reduce vortex-induced line vibrations with the objective to lower drag. During line drag measurements in the wind tunnel of the University of Graz, a tonal, flow-induced sound was observed. The tone was noticed to be associated with elevated drag regimes of the kite lines.

The phenomenon of flow-induced sound of flexible tethers was already known in the 17th century and used for the building of aeolian harps, a musical instrument played solely by the wind [26]. Despite this fact there are very limited investigations including data concerning the flow-induced sound of lightweight ropes or kite lines nor are there methods to specifically reduce flow-induced kite line noise. The object of our investigations was to understand the generation of flow-induced sound of kite lines and to develop an effective noise control method.

The major part of the paper is organized as follows: In Section 2, the general measurement setup and the investigated kite lines are described. Section 3 presents the experimental results and in Section 4 the sound radiation of kite lines in comparison to fixed cylinders is discussed.

2 Experimental design

2.1 Measurement setup

All of the investigations conducted were carried out in the aeroacoustic wind tunnel at the University of Erlangen-Nuremberg in Germany (Department of Sensor Technology and Institute of Fluid Mechanics). This closed-return type wind tunnel has an open working section of 4 m length surrounded by an anechoic chamber with 9 m by 6 m and a height of 3.6 m. The chamber itself has an

absorption coefficient of 0.9 for a frequency of 300 Hz and allows free-field acoustic measurements without reflections from the surrounding walls. The wind tunnel is provided with silencers to damp out fan noise and to make for a low noise level in the test section. Using an outlet nozzle with 0.2 m by 0.26 m (contraction ratio 6.3:1) the wind speed can be continuously controlled up to $U \leq 50 \text{ ms}^{-1}$. The flow velocity is determined by measuring the static pressure difference between the nozzle inlet and outlet and the current air density and the given contraction ratio of the nozzle. Several turbulence grids and a honeycomb decrease turbulence intensity down to 0.22% in the core of the jet [27]. Measurements have been performed at a room temperature of 21 °C and ambient pressure of approximately 1000 mbar.

As shown in Figure 1, the test object is attached to a mounting frame placed around the wind nozzle. Kite lines are placed centrally in the free jet and tensioned with weights to simulate the traction force produced by the kite. The distance between nozzle outlet and the vertically placed test object corresponds to the hydraulic nozzle diameter $d_h = 0.226 \text{ m}$. The line length between the upper and lower fixing point is 0.73 m.

Test objects are affected by two forces; the wind load in the flow direction and the tensile load that is adjusted to the specific line operating range. The tensile load provides the necessary force to hold the kite line straight and to prevent bowing deformation in the flow direction. In operation, the wind flow hits kite bridle lines at angles of attack of $45^\circ \leq \text{AOA} \leq 90^\circ$. Sound measurements of kite lines were made for these flow angles to gain information on the sound radiation of the complete set of kite bridle lines. The lower fixing point (see Fig. 1) has been moved downstream along the mounting rail (in positive x -direction) in order to reduce the AOA. Microphones have been positioned further downstream to keep exactly 1 m measuring distance.

The flow field to which the line length is exposed corresponds approximately to the nozzle height of 0.260 m. With a maximum line diameter of $D \leq 3.3 \text{ mm}$, the aspect ratio L/D is a minimum of 79, which exceeds the minimum recommended value of 50 to ensure two-dimensional flow condition [28]. The Reynolds number of the flow around the test object is determined by diameter and wind speed, changes of the kinematic air viscosity are negligible:

$$Re = \frac{UD}{\nu}. \quad (1)$$

The flow-induced noise is recorded in the anechoic chamber by four Brüel & Kjær type 4189 $\frac{1}{2}$ inch free field microphones. Figure 2 shows the microphone positions that are located at 1 m distance of the test object location indicated by the green dot. Microphones nr. 2 & 4 are positioned in the direction of the maximum sound radiation of a circular cylinder, perpendicular to flow direction and the cylinder/line axis [29]. Microphone nr. 1 & 3 are displaced by 22.5° from the main sound radiation direction to determine deviations in the directivity of the radiated sound and to investigate the dipolelike behaviour of tensioned kite lines. These acoustic measurements are carried out with no

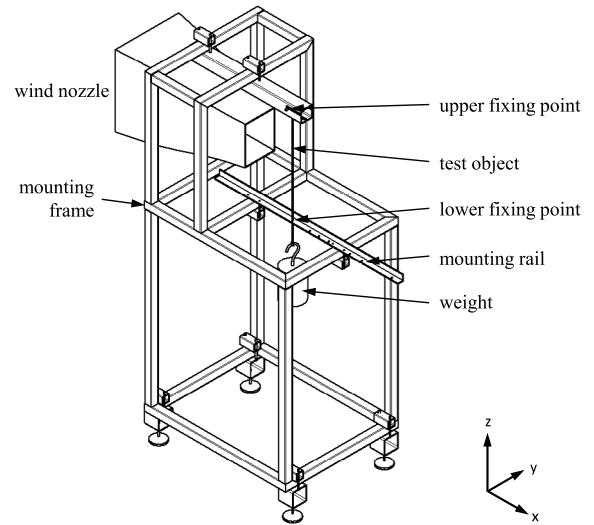


Figure 1. Mounting frame, isometric view.

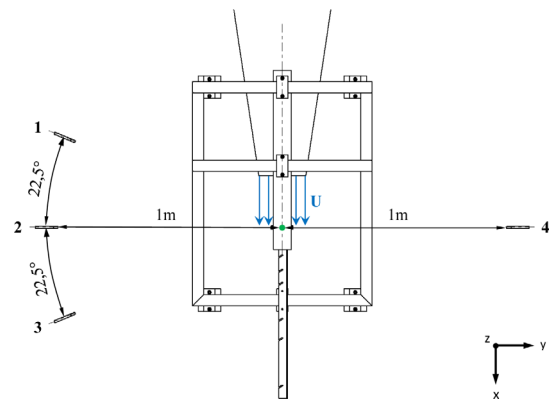


Figure 2. Measurement setup, top view.

obstructions other than the kite line itself present in the flow. Figure 3 displays the complete test rig. Frame components are covered with foam to avoid sound reflections in main sound propagation direction. At the lower fixing point, foam is pinched between test object and frame to prevent the transmission of vortex-induced vibrations (VIV) on to the steel frame.

Signals are amplified by a Nexus Conditioning Amplifier Type 2691 and recorded simultaneously with a PC using a LabView environment and a National Instruments PXIe 4497 data acquisition card. Measuring time is 30 s with a sampling frequency of 48 000 Hz. A Matlab routine is used to perform a fast Fourier transformation to compile the narrow band spectra with a Hanning window over 48 000 RMS values and 50% overlap. Subsequently an A-weighting filter is applied.

The overall sound pressure level (OASPL) is obtained by integrating the displayed noise spectrum from 100 Hz to 10 000 Hz. The length of the cylinder inside the flow increased with declining AOA, which according to Fujita et al. [30] among others will increase the radiated sound



Figure 3. Test rig, side view, AOA = 90°.

pressure level. This was corrected for by applying a factor as used by Latorre Iglesias et al. [14]:

$$\Delta\text{SPL}_{\Delta L} = -10\log_{10}(\Delta L) = 10\log_{10}(\sin(\theta)). \quad (2)$$

Here ΔL is the ratio between the cylinder effective length for angle of attack θ and the length at AOA 90°. The increasing aspect L/D for declining AOA can be neglected since two dimensional flow conditions are already ensured at $\theta = 90^\circ$.




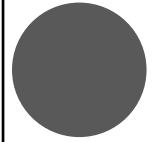
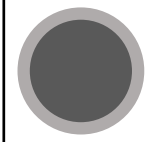
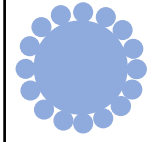
The Strouhal number St is calculated based on the frequency f_{St} corresponding to the peak sound pressure level (PSPL). The vortex shedding frequency and therefore the St -number is for AOA $\theta \geq 45^\circ$ directly proportional to the flow velocity component perpendicular to the cylinder axis according to the independence principle [13]:

$$St = \frac{f_{St} \cdot D}{U \cdot \sin(\theta)}. \quad (3)$$

2.2 Test objects

A principal test was conducted to compare the noise generated by a 3 mm wire rod, a kite line of the same diameter (Ref 1) and a M3 threaded rod. Table 1 shows the related test objects. The radiated sound of the wire rod is measured in order to gain basic knowledge about the sound radiation of rigid cylindrical objects under the given test conditions. In addition, the sound radiation of a threaded rod with M3 thread is measured to consider the effect of

Table 1. Characteristics of principal test objects.



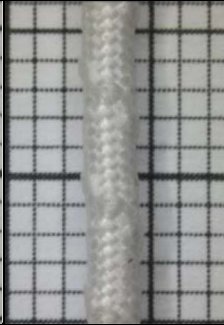


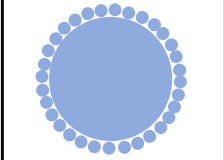
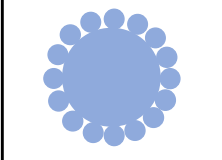
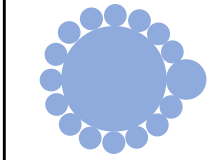
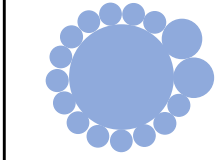
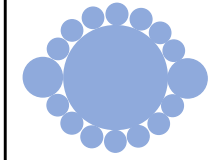
Image			
Name	Wire Rod	M3 Threaded Rod	Ref 1
Avg. Diam.	3.0 mm	2.675 mm	3.0 mm
Material, Construction	Steel, Cold-drawn	Steel, Cold-drawn	HMPE yarn core with 16 HMPE carrier sheath
Cross section			

greater surface roughness. All the investigated kite lines are made of high-modulus polyethylene (HMPE) fibres offering great yield strength at low density. The Ref 1 test item is constructed of a HMPE fibre core wrapped by a carrier sheath of 16 HMPE strands to protect the load-bearing fibre core. The kite line has a similar diameter of 3.0 mm under 50 kg tensile load. The 50 kg weight is attached to the line to simulate the tensile load of kite lines in operation.

A set of exploratory tests were carried out on test subjects constructed with braided sheath around core fibres to measure the influence of helical surface protrusions on radiated sound (Table 2). These kite lines are constructed of a HMPE fibre core wrapped by a braided HMPE carrier sheath. The Ref 2 test item is a heavy duty kite line with a bigger diameter and a tightly woven 32 HMPE carrier sheath. The sheath of the other kite lines is braided of 16 HMPE strands and a urethane coating is applied to reduce abrasive wear. The Helix lines are based on the concept where one of the strands of the braid has a greater diameter than the other carrier strands, whereby the resultant braid is one resembling a helical strake. The ratio of strake height to line diameter (h/D) is approximately 0.1, similar to strake sizes recommended in the literature [31].

The Helix lines are distinguished by number and width of the helical surface protrusion. The HMPE yarn core of the Ref 3 reference line is wrapped by 16 HMPE strands of similar denier and has a smooth surface.

Table 2. Characteristics of kite lines with yarn core; reference lines and kite lines with helical surface protrusions.

Image					
Name	Ref 2	Ref 3	Helix A	Helix B	Helix C
Average Diameter	3.3 mm	1.65 mm	1.85 mm	1.87 mm	1.87 mm
Material, Construction	HMPE yarn core with 32 HMPE carrier sheath	HMPE yarn core with 16 HMPE carrier sheath	HMPE yarn core with 16 HMPE carrier sheath	HMPE yarn core with 16 HMPE carrier sheath	HMPE yarn core with 16 HMPE carrier sheath
Helix Design	-	-	1 start; pitch $\lambda = 2D$ height $h = 0.1D$	1 wide start; pitch $\lambda = 2D$ height $h = 0.1D$	2 start; pitch $\lambda = 2D$ height $h = 0.1D$
Cross section					

Another set of exploratory tests were carried out for test items that were of a simple braid construction (no core). In Table 3, braided kite lines with 8 HMPE strands are displayed. The Ref 4 test item has a slightly larger diameter and is used as reference. The dissimilar trait of the Spiral is the double denier of one of its strands. The resultant braid forms a helical shaped line, like a stretched cork screw. The braiding of kite lines without yarn core allows greater helical strake pitch in comparison to the Helix lines shown in Table 2.

3 Results

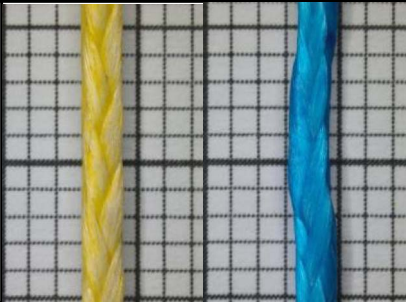


This section summarizes the flow-induced sound radiation of tensioned lines and the effect of helical surface protrusions on kite line noise control. Measurements are carried out at free stream velocities of $U = 10 \text{ ms}^{-1}$, 22 ms^{-1} and 34 ms^{-1} , resulting in Reynolds numbers of $800 \leq \text{Re} \leq 7270$, depending on line diameter. These three different wind speeds should allow a conclusion to be formed about the sound radiation of kite lines in the entire working range of crosswind kite generators.

The sound spectra depicted in this chapter are computed from the signal measured by microphone nr. 2 (see Fig. 2). The given sound pressure levels (PSPL and OASPL) are mean values computed from the signals of microphone nr. 2 and 4 which are placed in the main sound propagation direction. The presented Strouhal numbers are mean values calculated from all four microphone signals to reduce the influence of measurement deviations.

3.1 Comparison of flow-induced sounds of stiff cylinders and a tensioned tether

The far-field noise spectra of a smooth wire rod, a kite line of the same diameter and a threaded rod are compared to assess to what extent the aeroacoustic characteristics of stiff circular cylinders and a tensioned flexible tether correspond. The Ref 1 test item is tensioned with a 50 kg mass during measurements to hold the line and orient it perpendicular to the flow direction resulting in an angle of attack of 90° . Figure 4 shows the A-weighted sound pressure level of a 3 mm wire rod, a M3 threaded rod and the Ref 1 test item over a frequency range of 100 Hz to 10 000 Hz at different wind speeds. In all the following narrowband spectra,

Table 3. Characteristics of braided kite lines; reference line and kite line with helical shape.

Image		
Name	Ref 4	Spiral
Avg. Diam.	1.4 mm	1.2 mm
Material, Construction	8 HMPE carrier	8 HMPE carrier, 1 strand of double denier
Helix Design	-	1 start; pitch $\lambda = 9D$ height $h = 0.15D$
Cross section		

the inherent wind tunnel noise measured at these wind speeds is depicted in black since this is the lower limit for the acoustic measurements of objects in the free stream. Wind tunnel noise level increases with increasing flow velocity, mainly due to the sound generated by the mixing of the free jet and the static ambient air in the broadband region.

The narrowband spectra of the three test objects are similar and show one dominating peak representing the aeolian tone connected to air flow around cylindrical objects. This aeolian tone is perceptible as whistling with increasing volume and frequency for higher wind speeds. For higher wind speeds $U \geq 22 \text{ ms}^{-1}$ small side peaks occur at double and triple Strouhal frequency. For $f > f_{st}$ the sound pressure level decreases with 20 dB per order of frequency magnitude. The threaded rod generates significantly more aerodynamic sound as shown by the greater amplitude of its main and side peaks. The aeolian tone of the threaded rod has a higher frequency as the wire rod due to the smaller average diameter. The thread provides a higher surface roughness than the smooth cold-drawn wire rod, leading to greater boundary layer thickness [10]. The thicker boundary layer increases the diameter of the cylinder object in the flow and leads to the shedding of greater vortices at a lower frequency. This results in greater flow disturbance hence more aerodynamic sound (tonal and broadband noise) is generated.

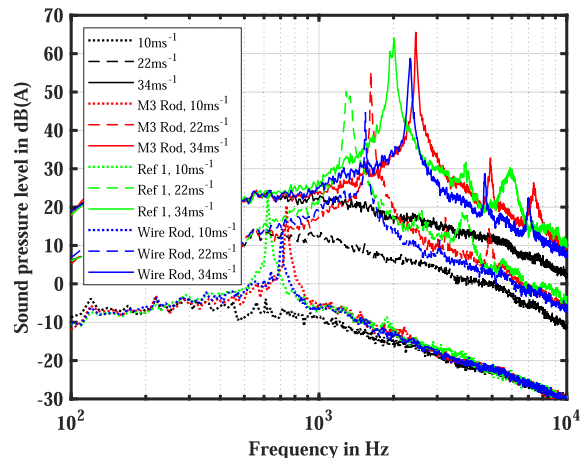


Figure 4. Flow-induced sound of the kite line Ref 1, a threaded rod and a wire rod in the narrowband spectrum.

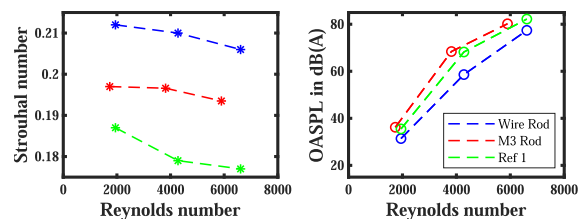


Figure 5. Strouhal number and Overall Sound Pressure Level of the kite line Ref 1, a threaded rod and a wire rod.

The aeolian tone of the Ref 1 test item has a lower frequency as the same diameter wire rod resulting in a smaller Strouhal number according to Formula (3). The peaks of the kite line are wider and have a greater amplitude compared to the peaks of the wire rod. Similarly as the wire rod, the kite line generates more aerodynamic sound due to its greater surface roughness. Unlike the stiff rods, the flexible line is excited to vibrate by the alternating pressures acting on the line during vortex shedding. The line vibration increases for higher wind speeds and causes vortex shedding with varying frequency resulting in wider main and side peaks in the sound spectra. The sharp peaks of the stiff rods are caused by the vortex shedding at constant Strouhal frequency.

Figure 5 shows the Strouhal number and the overall sound pressure level of the rods and the Ref 1 test item according to the Reynolds number. The measured Strouhal numbers of the wire rod correspond with literature values for smooth, round cylinders ($St \approx 0.21$) in this Reynolds range [32, 33]. As described above, a thicker boundary layer caused by greater surface roughness leads to the shedding of greater vortices with higher turbulence intensity [34] at a lower frequency [11]. This results in an averaged 6.5% smaller St value of the threaded rod and 13.5% lower Strouhal number of the kite line. For higher Reynolds numbers the Strouhal number of the test objects declines accordingly to published measurements of fixed, cross-flowed cylinders [35]. The greater surface roughness of the

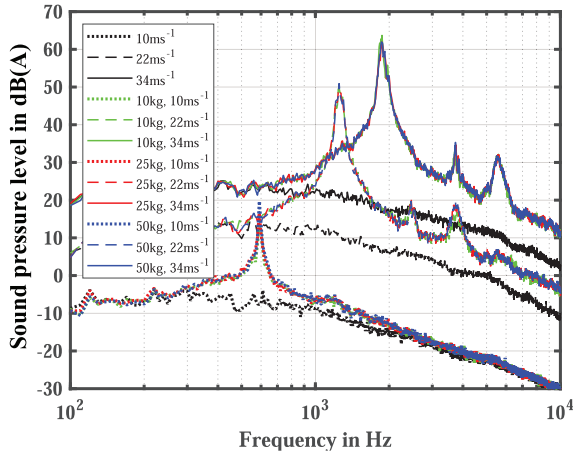


Figure 6. Flow-induced sound of a kite line Ref 2 tensioned with different line loads in the narrowband spectrum.

flexible kite line and the threaded rod lead to the generation of significantly more flow-induced sound compared to the rigid smooth wire rod. For increasing Re the OASPL rises to the same extent for these test objects. In general, fixed cylinders and tensioned kite lines show comparable aeroacoustic properties.

3.2 Influence of tensile load on flow-induced kite line noise

To investigate the influence of tensile load on the sound radiation of kite lines, the weight attached to the end of the line was varied. For this purpose, the radiated sound pressure of the test item Ref 2 was measured at a line tension load of 10, 25 and 50 kg at an AOA of 90° . Figure 6 shows that the narrowband spectra of the A-leveled sound pressure level does not change with varying tensile load. There is no measurable influence of the line tension load on the emitted sound pressure at any of the three flow velocities examined. The flow-induced sound radiation of the Ref 2 line is similar to the noise generated by the Ref 1 line.

Figure 7 shows the Strouhal number and the overall sound pressure level of the Ref 2 test item under different line loads according to the Reynolds number. The displayed values show, that the influence of the line tension load is negligibly small and has therefore not been considered further.

3.3 Influence of helical surface protrusions on flow-induced kite line noise

The flow-induced sound of the HMPE core kite lines with braided sheath and helical surface protrusions (see Table 2) developed by Dunker et al. [25] was measured and compared to the sound spectra of a reference line with similar construction and smooth surface (Ref 3). Figure 8 shows the A-leveled sound pressure level of these lines over a frequency of 100 Hz to 10 000 Hz at different wind speeds and various angles of attack. For low wind speeds ($U = 10 \text{ ms}^{-1}$) at AOA $\theta = 90^\circ$ the tonal peak of the kite

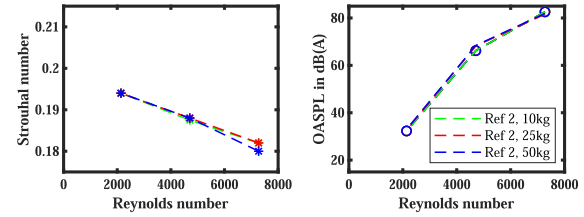


Figure 7. Strouhal number and Overall Sound Pressure Level of the kite line Ref 2 under different line loads.

lines with one helical surface protrusion (Helix A, Helix B) is suppressed and the radiated sound of these kite lines does hardly distinguish itself from the wind tunnel noise.

In comparison, the Ref 3 reference line and the Helix C with two helical surface protrusions, show a peak at their Strouhal frequency. For increasing wind speeds ($U \geq 22 \text{ ms}^{-1}$), more aeroacoustic sound is generated by all four core lines and the tonal peak of the Helix A and Helix B is not completely suppressed but amplitude and width of their tonal peak are significantly smaller compared to the Helix C and the reference line. The Helix C with two helical surface protrusions has a tonal peak at f_{St} and side peaks at double and triple Strouhal frequency and its sound spectra are comparable to the sound spectra of standard kite lines without spiral surface elevations.

The bigger diameter and the coarser surface of the Helix C lead to greater sound radiation at all investigated wind speeds compared to the smooth reference line Ref 3. Due to the small diameter of 1.87 mm, the Helix structure covers more than 50% of the Helix C surface, the gap between the surface protrusions is only 0.9 mm. It might be, that due to the small gap between the surface protrusions the upstream protrusion interfere with the flow of the second protrusion as observed by Nebres [36] and therefore generates significantly more aerodynamic sound than the Helix A line. Further investigations including boundary layer measurements are required to understand this phenomenon.

Sound measurements at AOA = 75° , 60° and 45° were conducted to examine the influence of the angle of attack on aeroacoustic noise of kite lines with helical surface protrusions. At $\theta \leq 75^\circ$ the sound spectra of all four core lines present a dominant, sharp peak at their Strouhal frequency. At $\theta = 90^\circ$ the tip of the peak is missing as in this case the lines with the attached weight hang straight down and are only slightly pressed against the notch in the mounting rail by the air flow. At smaller angles, the kite line is bent at the notch and presses against the mounting rail with greater force, thus the lower fixing point of the line is fastened much more tightly.

At $\theta = 75^\circ$ the 1-Start-Helix lines show significantly lower amplitude and width of the tonal peak than the Helix C and Ref 3. At $U \leq 22 \text{ ms}^{-1}$ the Helix A with its thinner spiral surface protrusion provides greater sound reduction compared to the Helix B. At $\theta = 60^\circ$ the 1-Start-Helix lines reduce tonal noise at $U = 10 \text{ ms}^{-1}$, for higher wind speeds only the side peaks are suppressed. At $\theta = 45^\circ$ there is no difference in the sound spectra of the three Helix lines and they show greater PSPL as the reference line at every

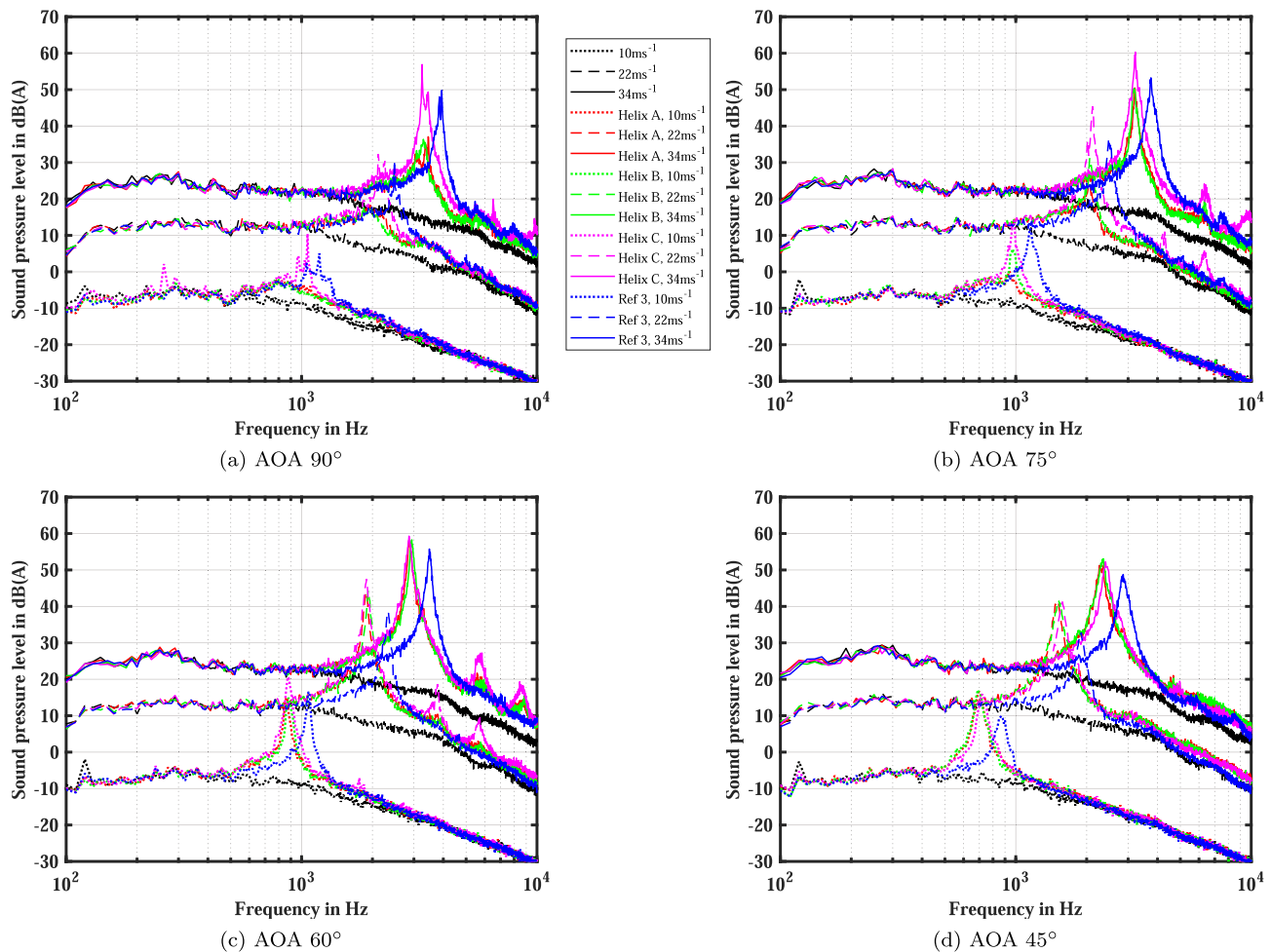


Figure 8. Flow-induced sound of kite lines with one (A & B) and two (C) helical surface protrusions and a reference line (Ref 3) in the narrowband spectrum at different wind speeds and angles of attack.

investigated wind speed. In Figures 8a–8d the decrease of the Strouhal frequency for smaller angles of attack according to Formula (3) is clearly visible.

Figure 9a shows the Strouhal number according to the angle of attack for the three different wind speeds. At 34 ms^{-1} the Strouhal numbers of all four core lines are constant for varying AOA. The Helix lines show generally smaller St values than the reference line because their coarser surface and the surface protrusions lead to a greater boundary layer thickness resulting in a bigger cylindrical object obstructing the wind flow and an eventual lower vortex shedding frequency. At 22 ms^{-1} and 10 ms^{-1} the effective noise suppression by the 1-Start-helix lines shows in lower Strouhal numbers for $\theta \geq 75^\circ$ as a result of the reduction of the tonal peak. Helix C and the Ref 3 have lower St values for increasing wind speeds as the Strouhal number of cylindrical objects decreases with increasing Reynolds number [35].

Figure 9b shows the overall sound pressure level according to the angle of attack for the three tested wind speeds. These are shown normalized to the case of the kite lines

normal to the flow as the length correction shown in Formula (2) has been applied. For $\theta = 60^\circ$ the Helix C and the smooth reference line Ref 3 generate maximum aerodynamic sound, higher and lower AOA result in lower noise generation. Helix A with its thinner surface protrusion shows slightly lower OASPL than the Helix B. In this diagram it is clearly visible how the noise reduction effect of the 1-Start-Helix is best at $\theta = 90^\circ$ and declines for decreasing AOA.

The reason for the decline in the sound-reducing effect lies in the geometric shape of the helical elevation. If the helix line is not placed exactly perpendicular to the flow direction, the pitch of the helical surface protrusion deviates on the opposite sides. As the angle of attack increases, the pitch becomes steeper on one side and flatter on the other. At an angle of attack of 45° , for the investigated pitch of $2D$, the surface protrusions run vertically on one side and horizontally on the right side (see Fig. 10). The helix should lead to a flow separation at different points of the line by means of its spiral-shaped elevations, so that the separation does not occur over the entire length shortly before the

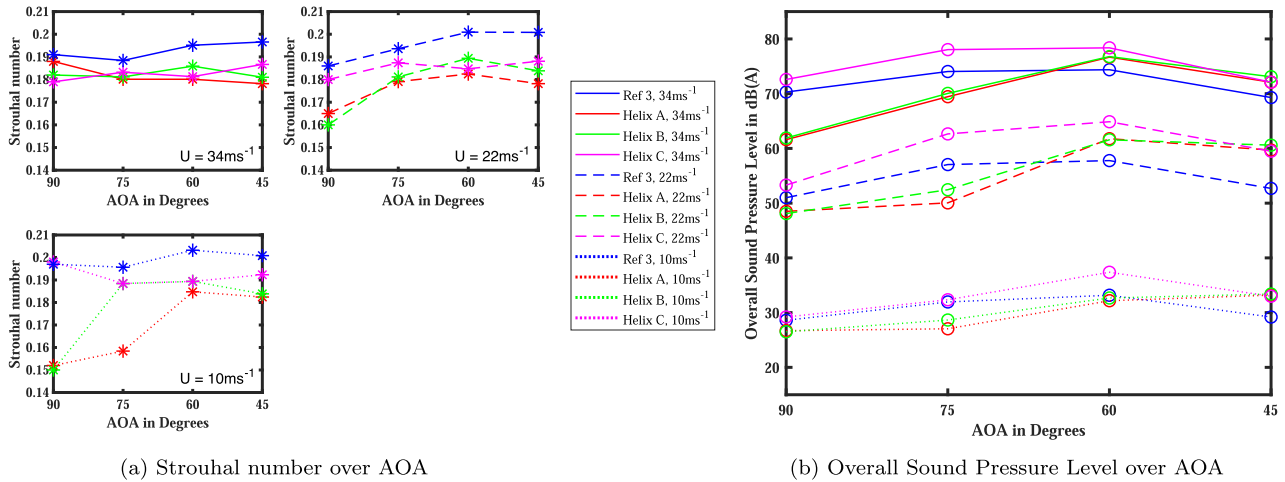


Figure 9. Strouhal number and overall sound pressure level of kite lines with one (A & B) and two (C) helical surface protrusions and a reference line (Ref 3) at different wind speeds and angles of attack.

thickest point of the line. This effect can obviously not be produced by an elevation that is perpendicular or horizontal to the flow, on the contrary this increases flow resistance and creates more flow disturbance.

3.4 Influence of helical line shape on flow-induced kite line noise

Sound measurements of the braided lines Spiral and Ref 4 were performed to investigate the influence of helical kite line shape on flow-induced sound of simple braid lines. Line load was reduced to 25 kg due to lower tensile strength of these lines. Figure 11 shows the A-weighted sound pressure level of the Spiral and the reference line in the range of 100 Hz to 10 000 Hz at different wind speeds ($U = 10, 22, 34 \text{ ms}^{-1}$) and various angles of attack.

If the Spiral is aligned perpendicular to the wind flow at $\theta = 90^\circ$, it generates broad band noise but does not create the typical aeolian tone. The helical line shape leads to a suppression of the tonal peak even at high wind speeds ($U = 34 \text{ ms}^{-1}$, $Re = 2650$) leading to 20 dB lower peak sound pressure level. The smooth reference line shows the typical sound spectra of a crossed-flown cylinder with a tonal peak at f_{st} and for $U \geq 22 \text{ ms}^{-1}$ additional side peaks at double and triple Strouhal frequency. For decreasing AOA the Spiral generates more tonal noise and the sound spectra assimilates to the sound spectra of the Ref 4. The noise suppression effect achieved through the helical line shape is reduced for decreasing AOA although on $\theta = 45^\circ$ the Spiral still radiates significantly less sound than the smooth reference line. The design of the Spiral shows the best results in reducing flow-induced sound of all investigated kite lines.

Figure 12a shows the Strouhal number of the Spiral and the Ref 4 according to the angle of attack for $U = 10 \text{ ms}^{-1}$, 22 ms^{-1} and 34 ms^{-1} . At $\theta = 90^\circ$ there is no detectable peak in the sound spectra of the Spiral and therefore no Strouhal number given. For $75^\circ \geq \theta \geq 45^\circ$ the Spiral has

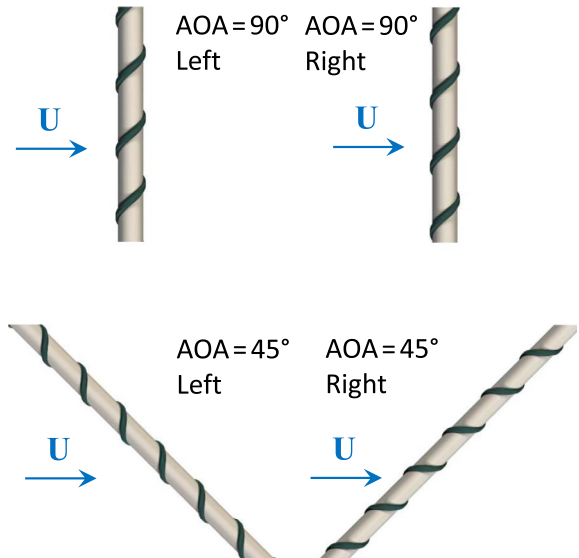


Figure 10. Path of a single helical surface protrusion of pitch $\lambda = 2D$ at an angle of attack of 90° and 45° .

an averagely 16% smaller Strouhal number compared to the Ref 4 due to the helical shape leading to a reduced vortex shedding frequency. Consistent with the results of Nebres and Batill [37], the greatest surface protrusion height leads to the lowest Strouhal number. Since the spiral has a 14% smaller diameter than Ref 4, the frequencies of the tonal peaks in Figures 11b–11d match. The sound reducing effect of the helical line shape decreases for lower AOA as can be seen in Figure 12b showing the overall sound pressure level according to the angle of attack for $U = 10 \text{ ms}^{-1}$, 22 ms^{-1} and 34 ms^{-1} . The results have been corrected for the different line lengths using the factor shown in Formula (2). The Spiral generates most aerodynamic sound at $\theta = 45^\circ$. The smooth reference line has the highest sound radiation at $\theta = 60^\circ$.

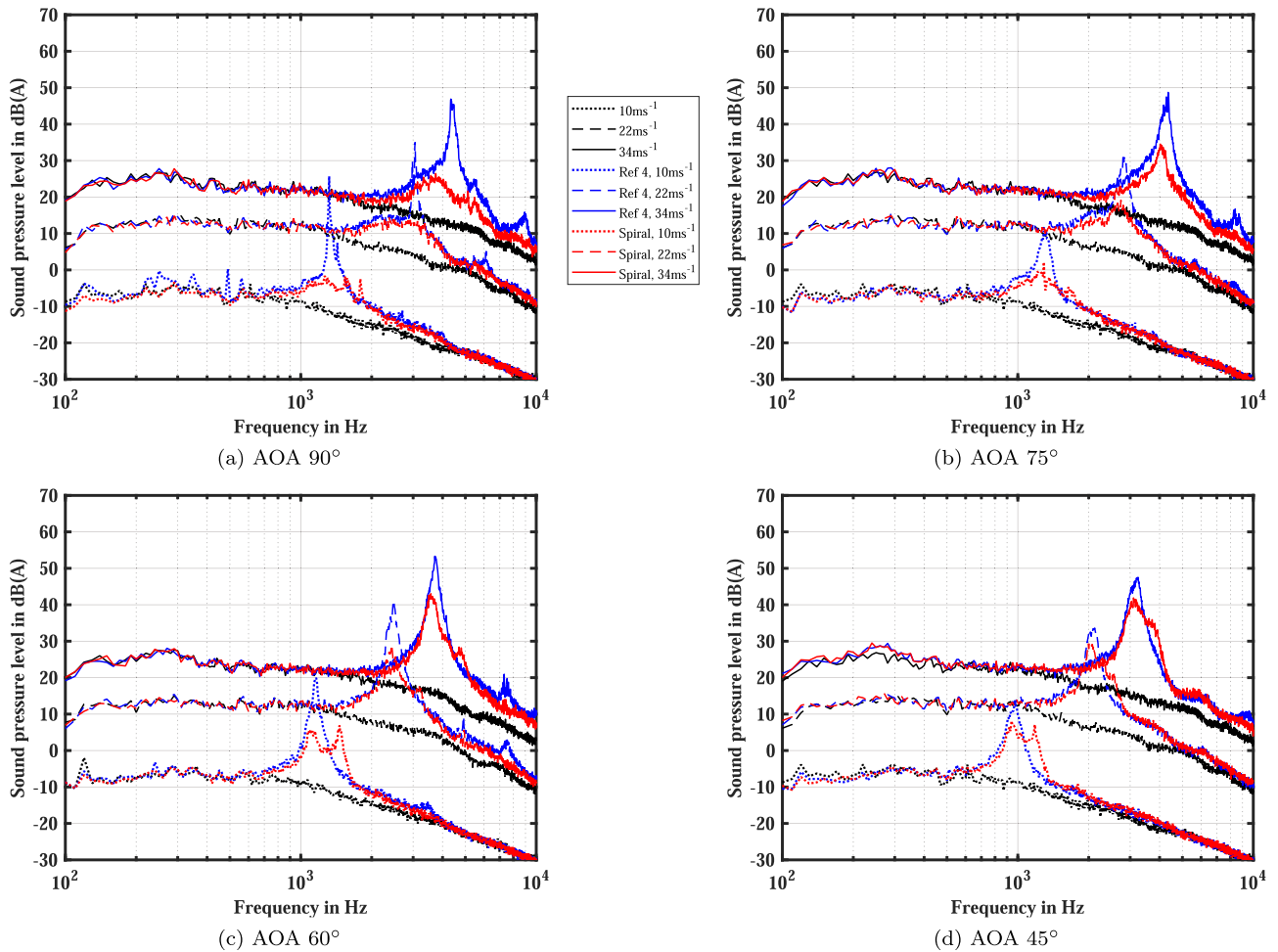


Figure 11. Flow-induced sound of a helical shaped kite line (Spiral) and a reference line (Ref 4) in the narrowband spectrum at different wind speeds and angles of attack.

4 Discussion

The kite lines without surface protrusions (Ref 1–4) show for $\text{AOA} = 90^\circ$ consistent Strouhal numbers in the range of $0.177 \leq \text{St} \leq 0.197$. The Strouhal number of cross-flowed lines as tensioned herein, is therefore about 10% smaller than the Strouhal number of circular cylinders in this Reynolds range, $0.20 \leq \text{St} \leq 0.21$ ($\text{AOA} = 90^\circ$) [32, 33, 35]). The aeroacoustic properties of rigid cylinders and tensioned lines also differ in the angle of attack at which the maximum sound radiation occurs. In the case of rigid smooth cylinders, sound radiation is at a maximum for $\theta = 90^\circ$ [14], while in the case of smooth kite lines this occurs around $\theta = 60^\circ$ although OASPL values are normalised accordingly to line length.

The threaded rod and the kite lines provide a higher surface roughness than the smooth cold-drawn wire rod leading to greater boundary layer thickness [10]. This leads to the shedding of larger vortices with higher turbulence intensity at lower frequency compared to fixed smooth cylinders with similar diameter [11, 34]. Accordingly the lower vortex shedding frequency results in lower Strouhal numbers and a

higher vorticity leads to greater sound radiation. Additionally the flow around the kite line is thought to interact with the vibrating line's surface causing varying vortex shedding frequencies and higher flow friction compared to smooth cylinders. The increased flow friction leads to even smaller Strouhal numbers compared to the threaded rod although the M3 thread provides the highest surface roughness of all investigated test objects. The Ref 2 test item has the highest bending stiffness due to its tightly woven sheath. This may contribute to a stronger resistance to VIV and could be a reason why it resulted in the highest St value of the tested kite lines. This corresponds to the findings of Dunker et al. [25].

Figure 13 illustrates the fundamental difference in the spreading wake area of smooth and helically-straked kite lines. The colours blue and red illustrate the different rotational direction of the vortices. The smooth kite line in the upper section of the image shows flow separation shortly before the thickest point of the body and a classic vortex street is formed in the wake area. The vortex formation zone starts shortly after the kite line and the width of the wake area exceeds the cylinder diameter by a factor of

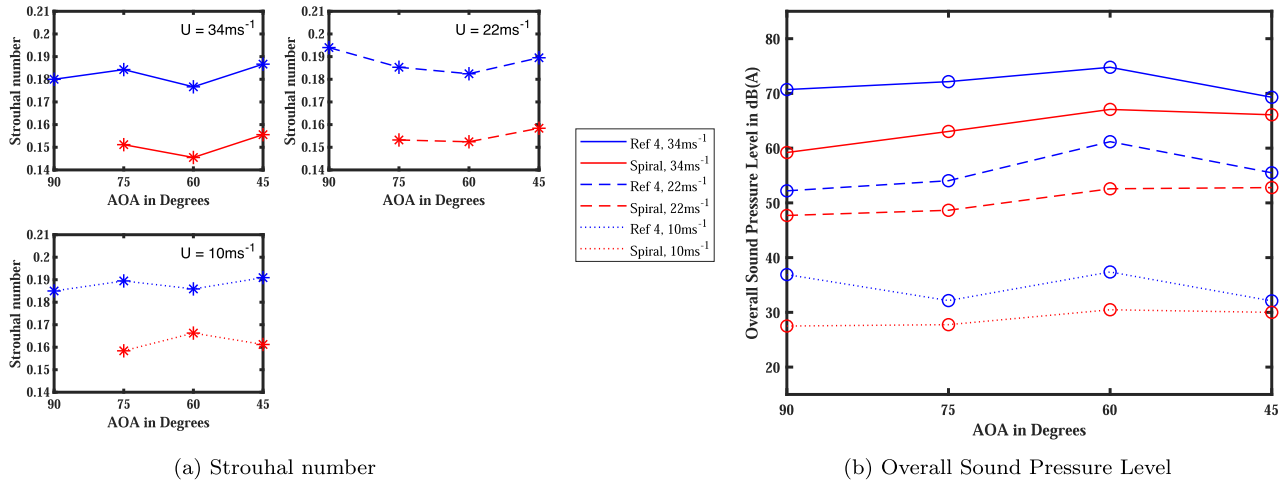


Figure 12. Strouhal number and overall sound pressure level of kite lines of a helical shaped kite line (Spiral) and a reference line (Ref 4) at different wind speeds and angles of attack.

several [8]. Spiral-shaped elevations cause a variation of the separation angle of the flow leading to pressure differences behind the test object. The resulting pressure field generates a secondary flow in the direction of the line axis behind cylindrical test object which shifts the vortex formation zone further downstream [19]. Additionally the variation of the separation angle reduces the vortex coherence along the cylinder axis, leading to a reduction in vortex size and intensity [20]. This results in decreasing pressure fluctuations on the line surface and in the wake area and therefore minimises tonal sound radiation [21].

The investigated lines are much thinner and more flexible compared to the rigid cylinders [21–23] considered in the literature. Therefore, the formation of a secondary flow behind the kite line is only possible to a limited extent. For increases in flow velocities, increases in line vibrations were observed. The increasing tonal noise of the helical straked kite lines at high flow velocities (see Figs. 8 and 9b) indicate that the line vibrations impact flow separation and impede the formation of the secondary flow.

The conducted experiments show that the aeroacoustic characteristics of fixed cylinders and tensioned lines are comparable. So the application of sound reduction measures that have been successfully tested on rigid cylinders are considered promising. Xing et al. [23] completely suppressed tonal cylinder noise using a helix with two spiral elevations of $\lambda = 2D$ pitch. In contrast, the kite line Helix C with two helical surface protrusions of similar pitch generated loud tonal noise. The surface protrusions cover more than 50% of the Helix C surface, the gap between the surface protrusions is only 0.9 mm. Due to the manufacturing process of the Helix lines the surface ratio of cylindrical base to helical protrusion as well as the curvature of the protrusions deviate strongly from the cylinders studied in the literature. Nigim and Batill [38] found that larger curvature of the surface protrusion lead to greater effect on flow disturbance. It can be concluded that the high surface proportion of the spiral-shaped elevations and the smooth transition between

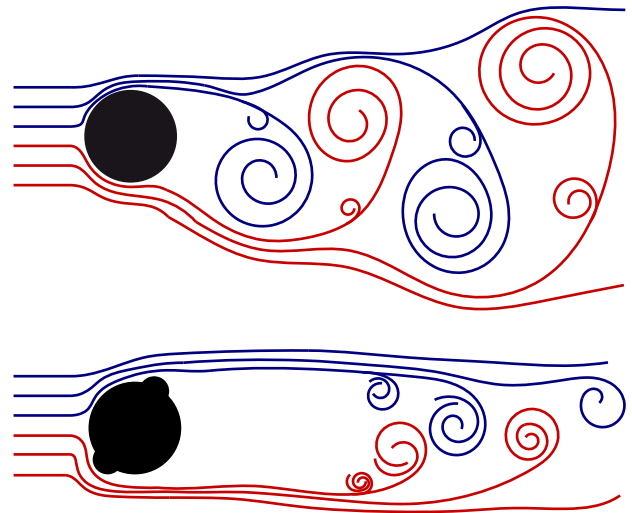


Figure 13. Schematic visualisation of the spreading wake area of cross-flow kite lines in top view [22, 37]. Top: Kite line without surface protrusion. Bottom: Kite line with 2 helical surface protrusions.

cylindrical core and the elevations lead to an insufficient influence on the flow separation. The sound spectra of the Helix C resembles the sound spectra of thicker kite lines without helical surface protrusion. In order to reduce line noise with the help of surface protrusions, the authors suggest to explore a relatively small portion of surface area, such as a $2D$ pitch and a sharp transition between line surface and protrusion.

No published results were found for the influence of varying angles of attack on the sound radiation of helical straked cylinders in cross-flow. Decreasing AOA lead to a reduction of the noise suppression effect of helical surface protrusions. Is the cylinder axis not aligned perpendicular to the flow direction, the helix pitch deviates on opposite

sides (see Fig. 10). A greater helix pitch might alleviate this issue, since the case that surface protrusions run vertically or horizontally is reached for lower AOA $\theta < 45^\circ$. With a greater helix pitch, however, the proportion of the line length where the detachment point is changed by the surface elevation also decreases. This in turn can lead to a reduction in the noise suppression effect and requires an additional surface elevation as seen in [23]. This geometric problem might be solved using a non-constant pitch adapted for the specific AOA. A varying helix pitch might be a good solution for fixed cylinders. For kite lines, omnidirectional measures are preferred since flexible lines can twist and their orientation to the incoming flow can vary. Helical shaped kite lines show generally better noise suppression than lines with helical surface protrusions. Similar to the helix lines, a decrease of the noise suppression is observed for lower AOA, although the aeolian tone of the helical line is significantly reduced even at $\theta = 45^\circ$.

Statements on the flow around and vibrational behaviour of kite lines can only be derived to a limited extent on the basis of the available measurement data and observations. Measurements of the line boundary layer by using a boundary layer probe and an investigation of the wake-velocity-field with particle image velocimetry or hot-wire anemometer can additionally verify the assumed correlations. Based on line vibration measurements the different source mechanisms of the sound radiation can be separated.

5 Conclusion

The sound radiation of kite lines has been investigated to develop an effective noise control method for crosswind kite energy systems. The experimental study extends the vast body of knowledge of flow about circular cylinders for Reynolds numbers $550 \leq \text{Re} \leq 7300$. The investigations carried out show that tensioned lines and rigid, thin cylinders have comparable aeroacoustic properties. Both radiate tonal sound and show a dominating peak in the sound spectrum at the specific Strouhal frequency. The study shows that helical surface protrusions also reduce aerodynamic sound of flexible cylindrical structures with small diameters.

Greater surface roughness causes higher sound radiation of cross-flow cylindrical objects and decreasing Strouhal numbers. Flexible lines generate more aerodynamic noise than rigid cylinders because lines are excited to vibrate by vortex shedding. Line tension has negligible influence on the sound radiation of kite lines in cross-flow.

If the kite line is aligned perpendicular to the flow direction (AOA = 90°) the sound radiation of kite lines with yarn core and braided sheath can be significantly reduced by a single helical surface protrusion. A single helix with $0.1D$ height and $2.6D$ pitch reduced the peak sound pressure level by up to 15 dB and the overall sound pressure level by up to 9 dB. For lower angles of attack, the noise suppression effect of helical surface protrusions with constant pitch decreases due to their geometrical shape.

Helical shaped kite lines show the best aeroacoustic properties of the tested cylindrical objects, since they enable

complete suppression of tonal kite line noise at AOA = 90° . In comparison to the straight reference line, the helical shape, of simple braid construction, reduces peak sound pressure level by up to 20 dB and overall sound pressure level by up to 11.5 dB. Even at AOA = 45° the helical line shape provides significant reduction of the aerodynamic noise although more sound is radiated for lower angles of attack similarly to lines with helical surface protrusions.

Conflict of interest

The authors declare that they have no conflicts of interest in relation to this article.

References

1. U. Zillmann, P. Bechtel: Airborne wind energy: Advances in technology development and research. Springer Berlin Heidelberg, Berlin, Heidelberg, 2018.
2. C. Vermillion, L. Fagiano: Electricity in the air: Tethered wind energy systems. ASME. Mechanical Engineering 135, 09 (2013) 13–21.
3. SkySails Power GmbH: Onshore unit sks pn-14. <https://skysails-power.com/onshore-unit-pn-14/>, 2022. Accessed: 2022-09-26.
4. V. Strouhal: Ueber eine besondere Art der Tonanregung. Annalen der Physik und Chemie 5 (1887) 216–251.
5. M.J. Lighthill: On sound generated aerodynamically: II. Turbulence as a source of sound. Proceedings of the Royal Society of London 222 (1954) 1–32.
6. H. Fujita: The characteristics of the aeolian tone radiated from two-dimensional cylinders. Fluid Dynamics Research 42, 1 (2010) 015002.
7. Y. Oguma, T. Yamagata, N. Fujisawa: Measurement of sound source distribution around a circular cylinder in a uniform flow by combined particle image velocimetry and microphone technique. Journal of Wind Engineering and Industrial Aerodynamics 118 (2013) 1–11.
8. L. Bösowirth, S. Bschorer: Technische Strömungslehre, Springer Vieweg Berlin Heidelberg, 10. auflage edition, 2014.
9. M.V. Morkovin: Flow around circular cylinder – a kaleidoscope of challenging fluid phenomena. American Society of Mechanical Engineering, 1964. Symposium on fully separated flows.
10. O. Güven, C. Farell, V.C. Patel: Surface-roughness effects on the mean flow past circular cylinders. Journal of Fluid Mechanics 98, 4 (1980) 673–701.
11. A. Alomar, D. Angland, X. Zhang, N. Molin: Experimental study of noise emitted by circular cylinders with large roughness. Journal of Sound and Vibration 333, 24 (2014) 6474–6497.
12. J.H. Gerrard: Measurements of the sound from circular cylinders in an air stream. *Proceedings of the Physical Society. Section B* 68, 7 (1955) 453–461.
13. M.M. Zdravkovich: Flow around circular cylinders – volume 1: Fundamentals. Journal of Fluids Engineering 120, 1 (1998) 216.
14. E. Latorre Iglesias, D.J. Thompson, M.G. Smith: Experimental study of the aerodynamic noise radiated by cylinders with different cross-sections and yaw angles. Journal of Sound and Vibration 361 (2016) 108–129.
15. S. Yamada, H. Fujita, Y. Maruty, H. Maki, J. Shiraishi: Experimental study on aerodynamic noise generated from two-dimensional models: 2nd report, effect of the angle of

- inclination of circular cylinders and the angle of attack of square cylinders to aerodynamic noise. Transactions of the Japan Society of Mechanical Engineers Series B 63, 610 (1997) 1974–1979.
16. Y. Haramoto, S. Yasuda, K. Matsuzaki, M. Munekata, H. Ohba: Analysis of aerodynamic noise generated from inclined circular cylinder. *Journal of Thermal Science* 9, 2 (2000) 122–128.
 17. W.F. King, B. Barsikow: An experimental study of sound generated by flow interactions with cylinders, 1999.
 18. T. Sueki, T. Takaishi, M. Ikeda, N. Arai: Application of porous material to reduce aerodynamic sound from bluff bodies. *Fluid Dynamics Research* 42 (2010) 015004.
 19. S.J. Lee, H.B. Kim: The effect of surface protrusions on the near wake of a circular cylinder. *Journal of Wind Engineering and Industrial Aerodynamics* 69–71 (1997) 351–361. Proceedings of the 3rd International Colloquium on Bluff Body Aerodynamics and Applications.
 20. J. Nebres, S. Batill: Flow about cylinders with helical surface protrusions. In 30th Aerospace Sciences Meeting and Exhibit, 6–9 January 1992, Reno, NV, USA, 1992: 01.
 21. L. Li, P. Liu, Y. Xing, H. Guo: Experimental investigation on the noise reduction method of helical cables for a circular cylinder and tandem cylinders. *Applied Acoustics* 152 (2019) 79–87.
 22. M. Razali, S.F. Zhou, L. Cheng: Experimental investigation on the mechanism of viv reduction using helical strakes. In Twentieth International Offshore and Polar Engineering Conference, 20–25 June 2010, Beijing, China. 2010.
 23. Y. Xing, P. Liu, H. Guo, L. Li: Effect of helical cables on cylinder noise control. *Applied Acoustics* 122 (2017) 152–155.
 24. K. Tsujimoto, S. Furukawa, K. Shimojima, K. Yamamoto: Development of ns-tacsr with extremely suppressed aeolian noise and its application to 500 kv overhead transmission line. *IEEE Transactions on Power Delivery* 6, 4 (1991) 1586–1592.
 25. S. Dunker, W. Meile, G. Brenn: Experiments in line vibration and associated drag for kites. In 23rd AIAA Aerodynamic Decelerator Systems Technology Conference, 30 Mar – 2 Apr 2015, Daytona Beach, FL. 2015.
 26. The Editors of Encyclopedia Britannica: Aeolian harp. <https://www.britannica.com/art/Aeolian-harp>, 2022. Accessed: 2022-09-26.
 27. R. Lerch, G. Sessler, D. Wolf: Technische Akustik. Springer-Verlag Berlin Heidelberg, 2009.
 28. C. Norberg: An experimental investigation of the flow around a circular cylinder: Influence of aspect ratio. *Journal of Fluid Mechanics* 258 (1994) 287–316.
 29. S. Becker, C. Hahn, M. Kaltenbacher, R. Lerch: Flow-induced sound of wall-mounted cylinders with different geometries. *AIAA Journal* 46, 9 (2008) 2265–2281.
 30. H. Fujita, W. Sha, H. Furutani, H. Suzuki: Experimental investigations and prediction of aerodynamic sound generated from square cylinders. In 4th AIAA/CEAS Aeroacoustics Conference, 2–4 June 1998, Toulouse, France. 1998, 2369 p.
 31. M.M. Zdravkovich: Review and classification of various aerodynamic and hydrodynamic means for suppressing vortex shedding. *Journal of Wind Engineering and Industrial Aerodynamics* 7, 2 (1981) 145–189.
 32. C.C. Cardell: *Flow past a circular cylinder with a permeable wake splitter plate*. PhD thesis, California Institute of Technology, 1993.
 33. L. Ong, J. Wallace: The velocity field of the turbulent very near wake of a circular cylinder. *Experiments in Fluids* 20 (1996) 441–453.
 34. W.M. Chakroun, A.A. Abdel Rahman, M.M.A. Quadri: The effect of surface roughness on flow around a circular cylinder. *Wind Engineering* 21, 1 (1997) 1–12.
 35. R.D. Blevins: Flow-induced vibration. Krieger Publishing Company, 2001.
 36. J. Nebres: Wake similarity and vortex formation for two-dimensional bluff bodies. PhD thesis, University of Notre Dame, Indiana, 1992.
 37. J. Nebres, S. Batill: Flow about a circular cylinder with a single large-scale surface perturbation. *Experiments in Fluids* 15 (1993) 369–379.
 38. H.H. Nigim, S.M. Batill: Flow about cylinders with surface perturbations. *Journal of Fluids and Structures* 11, 8 (1997) 893–907.

Cite this article as: Saur L. Riedel J. Dunker S. & Becker S. 2023. Experimental investigation of flow-induced sound of kite lines. *Acta Acustica*, 7, 35.